Structure
Article

CdiA from *Enterobacter cloacae* Delivers a Toxic Ribosomal RNase into Target Bacteria

Christina M. Beck,[1,5] Robert P. Morse,[2,5] David A. Cunningham,[1] Angelina Iniguez,[2] David A. Low,[1,3] Celia W. Goulding,[2,4] and Christopher S. Hayes[1,3,*]

[1]Department of Molecular, Cellular, and Developmental Biology, University of California, Santa Barbara, Santa Barbara, CA 93106-9625, USA
[2]Department of Molecular Biology and Biochemistry, University of California, Irvine, Irvine, CA 92697, USA
[3]Biomolecular Science and Engineering Program, University of California, Santa Barbara, Santa Barbara, CA 93106-9625, USA
[4]Department of Pharmaceutical Sciences, University of California, Irvine, Irvine, CA 92697, USA
[5]Co-first authors
*Correspondence: chayes@lifesci.ucsb.edu
http://dx.doi.org/10.1016/j.str.2014.02.012

SUMMARY

Contact-dependent growth inhibition (CDI) is one mechanism of inter-bacterial competition. CDI$^+$ cells export large CdiA effector proteins, which carry a variety of C-terminal toxin domains (CdiA-CT). CdiA-CT toxins are specifically neutralized by cognate CdiI immunity proteins to protect toxin-producing cells from autoinhibition. Here, we use structure determination to elucidate the activity of a CDI toxin from *Enterobacter cloacae* (ECL). The structure of CdiA-CT^{ECL} resembles the C-terminal nuclease domain of colicin E3, which cleaves 16S ribosomal RNA to disrupt protein synthesis. In accord with this structural homology, we show that CdiA-CT^{ECL} uses the same nuclease activity to inhibit bacterial growth. Surprisingly, although colicin E3 and CdiA^{ECL} carry equivalent toxin domains, the corresponding immunity proteins are unrelated in sequence, structure, and toxin-binding site. Together, these findings reveal unexpected diversity among 16S rRNases and suggest that these nucleases are robust and versatile payloads for a variety of toxin-delivery platforms.

INTRODUCTION

Bacterial genomes and plasmids encode a variety of peptide and protein toxins that mediate inter-bacterial competition. Colicins were the first of such toxins to be identified and characterized from strains of *Escherichia coli*. Subsequently, it was discovered that other bacteria release similar toxins, which are now collectively termed bacteriocins (Cascales et al., 2007). Bacteriocins are diffusible proteins that parasitize cell-envelope proteins to enter and kill bacteria. These toxins are composed of three domains, each responsible for a distinct step in the cell-killing pathway. The central domain binds specific receptors on the surface of susceptible bacteria. The N-terminal domain mediates translocation across the cell envelope, and the C-terminal domain carries the bacteriocidal activity. This modular structure allows for delivery of diverse C-terminal toxins using conserved translocation and receptor-binding domains. For example, colicins E2 through E9 share virtually identical N-terminal domains but carry different C-terminal toxins with DNase (Schaller and Nomura, 1976), ribosomal RNase (Bowman et al., 1971; Senior and Holland, 1971), or tRNA anticodon nuclease activities (Ogawa et al., 1999). Bacteriocin genes are always closely linked to immunity genes, which encode small proteins that specifically bind and neutralize the toxin domains. Thus, cells that harbor bacteriocinogenic plasmids are protected from toxin activity, but they may still be susceptible to the bacteriocins produced from other plasmids. Many different bacteriocin/immunity types are typically present in a given environment (Gordon et al., 1998; Riley and Gordon, 1992), and these plasmids are predicted to have a significant impact on bacterial population structures (Chao and Levin, 1981; Czárán et al., 2002).

Research over the past decade has uncovered additional bacterial competition systems that require direct cell-to-cell contact for toxin delivery (Aoki et al., 2005, 2010; Hood et al., 2010; MacIntyre et al., 2010; Zheng et al., 2011). There are at least two pathways—mediated by type V and type VI secretion systems—for contact-dependent toxin delivery between Gram-negative bacteria (Ruhe et al., 2013a; Silverman et al., 2012). The type V mechanism was the first identified, and this phenomenon was termed "CDI" for *c*ontact-*d*ependent growth *i*nhibition (Aoki et al., 2005). CDI is mediated by the CdiB/CdiA family of two-partner secretion proteins. CdiB is a predicted β-barrel protein that resides in the outer membrane and is required for export of CdiA effectors. CdiA proteins are very large (250–600 kDa) and are thought to extend from the inhibitor cell to interact with neighboring target bacteria. Although CdiA and bacteriocins are unrelated, these effector proteins share a number of general features. Like bacteriocins, CdiA proteins bind to specific receptors on the surface of target bacteria, and these interactions determine the target-cell range (Aoki et al., 2008; Ruhe et al., 2013b). Additionally, CDI toxin activity is carried at the extreme C terminus of CdiA, and some portion of this CdiA-CT region is translocated into target bacteria (Aoki et al., 2010; Morse et al., 2012; Webb et al., 2013). CDI loci also encode CdiI immunity proteins, which bind and inactivate CdiA-CTs to protect toxin-producing cells from autoinhibition. Finally, CDI systems deploy a variety of toxin domains with distinct biochemical activities. Remarkably, chimeric CDI effectors can be produced by fusing different toxins onto CdiA at the conserved VENN peptide motif that demarcates the

CdiA-CT region (Aoki et al., 2010). There is also evidence that bacteria exchange *cdiA-CT/cdiI* genes through horizontal transfer (Poole et al., 2011), suggesting that effector modularity is exploited to switch toxin/immunity type. In fact, bacteria collectively contain a large repository of toxin/immunity genes that are shared by a variety of toxin-delivery systems (Holberger et al., 2012; Poole et al., 2011; Zhang et al., 2011, 2012). For example, at least two CdiA proteins carry toxins with homology to bacteriocin nucleases. CdiA^{Dd3937} from *Dickeya dadantii* 3937 carries a CT domain with 35% identity to the pyocin S3 DNase domain (Aoki et al., 2010), and the C-terminal region of CdiA^{K96243} from *Burkholderia pseudomallei* K96243 is 49% identical to the anticodon tRNase domain of colicin E5. Biochemical analyses have confirmed that each of these CDI toxins has the same nuclease activity as the corresponding bacteriocin (Aoki et al., 2010; Nikolakakis et al., 2012). Together, these observations suggest that CDI loci integrate toxin/immunity gene pairs from diverse sources and that this diversity contributes to inter-strain competition.

In an effort to understand CDI toxin/immunity diversity and uncover toxin activities, we have initiated structural studies of CdiA-CT/CdiI pairs from various bacteria. Here, we describe the structure and function of the CDI toxin/immunity protein pair from *Enterobacter cloacae* ATCC 13047 (ECL). The CdiA-CT^{ECL} toxin shares no significant sequence identity with proteins of known function, but the three-dimensional structure of CdiA-CT^{ECL} reveals similarity to the C-terminal nuclease domain of colicin E3. In accordance with the structural homology, CdiA-CT^{ECL} cleaves 16S rRNA at the same site as colicin E3, and this nuclease activity is responsible for growth inhibition. By contrast, CdiI^{ECL} does not resemble the colicin E3 immunity protein (ImE3), and the two immunity proteins bind to different sites on their respective cognate toxin domains. Inspection of other CdiA proteins from *Erwinia chrysanthemi* EC16 (Uniprot ID code P94772), *Enterobacter hormaechei* ATCC 49162 (Uniprot ID code F5S237), and *Pseudomonas viridiflava* UASWS0038 (Uniprot ID code K6CF79) has revealed that their toxin domains share a common nuclease motif with colicin E3 (Walker et al., 2004). Analysis of CdiA-CT^{EC16} from *Erwinia chrysanthemi* EC16 confirms that this toxin has 16S rRNase activity and demonstrates that the associated CdiI^{EC16} immunity protein is specific to CdiA-CT^{EC16} and does not provide protection against the CdiA-CT^{ECL} nuclease. Together, these observations indicate that 16S rRNase toxins are more diverse and widespread than previously recognized.

RESULTS

Crystallization and Structure of the CdiA-CT^{ECL}/CdiI^{ECL} Complex

In a previous study, we used structural analysis to determine the activities of CDI toxins from *E. coli* EC869 and *B. pseudomallei* 1026b (Morse et al., 2012). Because the CDI toxin/immunity pair from *E. cloacae* ATCC 13047 shares no sequence homology with proteins of known function, we followed a similar structure-based approach to characterize this system. The CdiA-CT^{ECL} region is demarcated by the AENN peptide motif and corresponds to residues Ala3087 to Asp3321 of full-length CdiA^{ECL}. We coexpressed CdiA-CT^{ECL} with His$_6$-tagged CdiI^{ECL} and purified the complex to near homogeneity (Figure S1A available online). The N-terminal region of CdiA-CT^{ECL} was partially degraded during crystallization (Figure S1A), presumably because this region is disordered. Similar N-terminal degradation has been observed with other CdiA-CTs (Morse et al., 2012). The CdiA-CT^{ECL}/CdiI^{ECL} complex crystallized in space group $P4_122$ with one heterodimeric complex per asymmetric unit (Figure S1B). The structure was solved by selenium multiple wavelength anomalous dispersion (Se-MAD) phasing to 2.4 Å resolution. The final refined model contains CdiA-CT^{ECL} residues 160–235 (numbered from Ala1 of the AENN motif) and CdiI^{ECL} residues 1–145. In addition, 62 well-resolved water molecules are included in the final model, resulting in a R_{work}/R_{free} of 18.3/23.7 (Table 1).

The resolved C-terminal domain of CdiA-CT^{ECL} consists of an N-terminal α helix, followed by a twisted five-stranded antiparallel β sheet (Figure 1A). The domain contains two long loops, L2 and L4, which connect β1 to β2 and β3 to β4, respectively (Figure 1A). Weak electron density was observed for loop L4, likely because of its flexibility, and thus Ser206–Asn211 were modeled as alanine residues. The CdiI^{ECL} immunity protein comprises three- and four-stranded antiparallel β sheets, forming a β sandwich that is decorated with three α helices (Figure 1A). The toxin and immunity protein interface is elaborate and mediated by a series of hydrogen-bond (H-bond), electrostatic, and hydrophobic interactions (Figures 1B; Table S1). CdiA-CT^{ECL} residues within loops L2–L6 form H-bonds and ion-pair interactions with CdiI^{ECL} residues in loops L1′, L2′, and L3′ and the edge of the β sandwich (β3′, β5′, and β6′) (Figure 1B). A water-mediated network of H-bonds also contributes to the interface, resulting in more than 20 ion-pair/H-bond interactions between toxin and immunity proteins (Figure 1B; Table S1). In addition, there is a hydrophobic interface of approximately 300 Å^2 consisting of Ile178, Val192, Tyr199, and Phe216 from CdiA-CT^{ECL}, and Phe76, Phe78, Val95, and Phe97 from CdiI^{ECL} (Figure 1C). Overall, the CdiA-CT^{ECL}/CdiI^{ECL} complex has an interface of 1,399 Å^2, burying 27.6% and 17.1% of the solvent-accessible surface areas of the toxin and immunity proteins, respectively.

CdiA-CT^{ECL} Is Structurally Homologous to the Nuclease Domain of Colicin E3

CdiA-CT^{ECL} shares no structural homology with previously characterized CDI toxins from *E. coli* EC869 and *B. pseudomallei* 1026b (Morse et al., 2012; Nikolakakis et al., 2012). Searches for structural homologs using the DALI server (Holm and Rosenström, 2010) revealed that CdiA-CT^{ECL} is similar to the C-terminal nuclease domain of colicin E3 (ColE3-CT). Colicin E3 is a plasmid-encoded bacteriocin found in some *E. coli* strains, and its nuclease domain cleaves 16S rRNA between residues A1493 and G1494 (*E. coli* numbering) to interfere with protein synthesis (Lancaster et al., 2008; Ng et al., 2010). The CdiA-CT^{ECL} and ColE3-CT domains share a twisted antiparallel β sheet and superimpose with a root-mean-square deviation (rmsd) of 2.1 Å over 76 α carbons, corresponding to a *Z* score of 4.8, whereas the sequence identity between the two domains is approximately 18% (Figures 2A and S2A). Residues Asp510, His513, and Glu517 of colicin E3 are thought to function

Table 1. Crystallographic Statistics for the CdiA-CT^{ECL}/CdiI^{ECL} Protein Complex

	Peak	Remote	Inflection	Native
Space group	$P4_122$	$P4_122$	$P4_122$	$P4_122$
Unit cell dimensions (Å)	85.64 85.64 75.17	85.64 85.64 75.17	85.64 85.64 75.17	85.25 85.25 74.91
pH of crystallization condition	5.1	5.1	5.1	5.1
Protein concentration (mg/ml)	9	9	9	9
Data set				
Wavelength (Å)	0.9759	1.377	0.9794	1
Resolution range	50–2.85	50–3.0	50–2.9	50–2.4
Unique reflections (total)	5,486 (191,798)	4,645 (163,018)	5,179 (181,470)	11,315 (324,387)
Completeness (%)[a]	100.0 (100.0)	100.0 (100)	100.0 (100.0)	100 (100)
Redundancy [a]	27.8 (28.8)	27.6 (28.5)	27.8 (28.7)	28.7 (29.3)
R_{merge} [a,b]	0.114 (0.47)	0.129 (0.501)	0.109 (0.445)	0.088 (0.455)
I/σ[a]	31.1 (10.42)	27.8 (8.7)	34.8 (10.8)	44.7 (11)
NCS copies	1			1
No. of selenium sites/a.u.	6			
Figure of merit	0.49			
Model refinement				
Resolution range (Å)				38.125–2.400
No. of reflections (working/free)				11,291/538
No. of protein atoms				1760
No. of water molecules				62
Missing residues				CdiA-CT 1-159
R_{work}/R_{free}[c] (%)				18.3/23.7
Rmsd				
Bond lengths (Å)				0.008
Bond angles (degrees)				1.15
Ramachandran plot				
Most favorable region (%)				93.61
Additional allowed region (%)				6.39
Disallowed region				0.0
PDB ID code				4NTQ

[a]Statistics for the highest-resolution shell are given in brackets.
[b]$R_{merge} = \Sigma|I - < I > |/\Sigma I$.
[c]$R_{work} = \Sigma|F_{obs}\text{-}F_{calc}|/\Sigma F_{obs}$ R_{free} was computed identically, except where all reflections belong to a test set of 10% randomly selected data.

directly in catalysis (Ng et al., 2010; Soelaiman et al., 2001; Walker et al., 2004), and CdiA-CT^{ECL} residues Asp203, Asp205, and Lys214 superimpose upon these colicin E3 active-site residues (Figures 2B and S2A). Together, these structural similarities suggest that CdiA-CT^{ECL} may share 16S rRNA nuclease activity with colicin E3.

Although the CdiA-CT^{ECL} and ColE3-CT toxin domains are structurally similar, the corresponding immunity proteins are not related to one another in either primary or tertiary structure (Figures S3A and S3B). The colicin E3 immunity protein (ImE3) is significantly smaller than CdiI^{ECL} (~9.9 versus 16.9 kDa), and the two proteins have different folds (Figure S3B). A DALI search reveals that CdiI^{ECL} is most similar to the Whirly family of single-stranded DNA binding proteins (Desveaux et al., 2005). The closest structural homologs are two proteins of unknown function from cyanobacteria (Protein Data Bank [PDB] ID codes 2IT9 and 2NVN), which superimpose onto CdiI^{ECL} with rmsds of 3.6–4.0 Å over 120–122 α carbons (Figure S3C). CdiI^{ECL} and ImE3 also bind their cognate toxins differently. ImE3 binds to an "exosite" that leaves the colicin E3 active site exposed (Carr et al., 2000), whereas CdiI^{ECL} binds directly over the predicted active site (Figure 2C). Structural alignment of the complexes shows that immunity protein binding occurs at distinct non-overlapping positions (Figure 2D). Interestingly, ColE3-CT contains a C-terminal extension not found in CdiA-CT^{ECL} (Figure 2A). This C-terminal tail forms a short α helix in one ColE3-CT structure (Soelaiman et al., 2001), and this element would likely interfere with CdiI^{ECL} binding were it present in CdiA-CT^{ECL}. Similarly, the orientation of loop L2 differs considerably between the toxins (Figure 2A), and these loops could block the binding of non-cognate immunity proteins (Figure 2D). Despite these differences, each immunity protein is predicted to prevent its cognate toxin from entering the ribosome A site (Figures S4) (Ng et al., 2010), and therefore toxin inactivation is fundamentally the same for both systems.

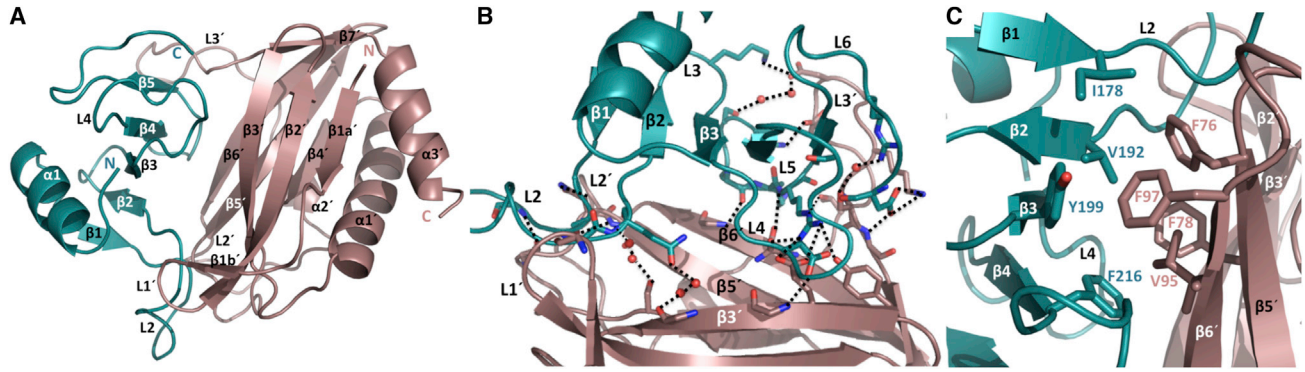

Figure 1. Structure of the CdiA-CT/CdiI^{ECL} Complex

(A) The CdiA-CT^{ECL} toxin (teal) and CdiI^{ECL} immunity protein (salmon pink) are depicted in ribbon representation with secondary structure elements. The amino and carboxyl termini are indicated by (N) and (C), respectively. CdiI^{ECL} elements are denoted with a prime symbol (′) to differentiate them from the toxin secondary structure elements.

(B) The CdiA-CT/CdiI^{ECL} interface is mediated by an extensive network of ion-pair and H-bond interactions. Interacting residues are shown as sticks with oxygen, and nitrogen atoms are colored red and blue, respectively. Water molecules are depicted as red spheres, and interacting bonds are depicted as black dotted lines.

(C) The CdiA-CT/CdiI^{ECL} interface also contains hydrophobic interactions mediated by the residues indicated in one-letter code. The view in (B) represents a 90° clockwise rotation of (A) and (C).

Also see Figure S1.

CdiA-CT^{ECL} Cleaves 16S rRNA In Vivo to Inhibit Cell Growth

The structural resemblance of CdiA-CT^{ECL} to ColE3-CT suggests that the CDI toxin also cleaves 16S rRNA. To test this prediction, we cloned *cdiA-CT*^{ECL} under the control of an arabinose-inducible promoter and asked whether 16S rRNA is cleaved upon induction with L-arabinose. *E. coli* cells carrying the *cdiA-CT*^{ECL} construct do not grow when the media is supplemented with L-arabinose (Figure 3A), confirming that CdiA-CT^{ECL} is an inhibitory toxin. We isolated total RNA from the inhibited cells and analyzed 16S rRNA by northern blot. This analysis revealed that 16S rRNA is cleaved in cells expressing *cdiA-CT*^{ECL} but remains intact in control cells that carry the vector plasmid alone (Figure 3B). We next tested CdiI^{ECL} function to determine whether it neutralizes the growth inhibition and nuclease activities of CdiA-CT^{ECL}. We cloned *cdiI*^{ECL} under the control of an isopropyl β-D-1-thiogalactopyranoside-inducible promoter and introduced the resulting plasmid into cells that harbor the arabinose-inducible *cdiA-CT*^{ECL} construct. Cells expressing both *cdiA-CT*^{ECL} and *cdiI*^{ECL} grow at the same rate as control cells that carry empty vector plasmids (Figure 3A), indicating that CdiI^{ECL} prevents CdiA-CT^{ECL}-mediated growth inhibition. Furthermore, northern analysis shows that 16S rRNA is not cleaved in cells that coexpress *cdiA-CT*^{ECL} and *cdiI*^{ECL} (Figure 3B), demonstrating that the immunity protein also blocks nuclease activity. Together, these results show that CdiA-CT^{ECL} and CdiI^{ECL} constitute a cognate toxin/immunity pair that targets the ribosome.

CdiI^{ECL} Immunity Function Is Specific for Its Cognate Toxin

At least one other CdiA protein is predicted to possess 16S rRNase activity. Walker et al. (2004) discovered that HecA from *Erwinia chrysanthemi* EC16 contains the same catalytic motif as colicin E3 (Figure S2B). HecA was originally identified as an adhesin that promotes bacterial colonization of plant hosts (Rojas et al., 2002, 2004), but this protein shares 68% sequence identity with a known CdiA effector (Uniprot ID code E0SCQ6) from *Dickeya dadantii* 3937 (Aoki et al., 2010). Together, these observations suggest that HecA actually functions in CDI, and therefore we refer to this protein as CdiA^{EC16}. To test toxin activity, we cloned the *cdiA-CT*^{EC16} sequence under control of an arabinose-inducible promoter for expression in *E. coli* cells. As predicted, cell growth is inhibited when *cdiA-CT*^{EC16} expression is induced (Figure 3C), and northern analysis shows 16S rRNA cleavage in the inhibited cells (Figure 3D). Because CDI systems are always arranged as toxin/immunity gene pairs, we tested the small open reading frame found immediately downstream of *cdiA*^{EC16} for immunity function. The predicted *cdiI*^{EC16} gene blocks the growth inhibition and nuclease activities associated with *cdiA-CT*^{EC16} expression (Figures 3C and 3D). CdiA-CT^{EC16} and CdiI^{EC16} do not share significant sequence identity with the toxin/immunity proteins from *E. cloacae* (Figure S2; data not shown), suggesting that each immunity protein is specific for its cognate toxin. Indeed, we found that *cdiI*^{ECL} and *cdiI*^{EC16} only protect cells from the inhibitory effects of their corresponding toxins (Figures 3A and 3C). Similarly, each immunity gene specifically blocks the nuclease activity associated with its cognate toxin (Figures 3B and 3D). Thus, although CdiA-CT^{ECL} and CdiA-CT^{EC16} share a common growth inhibition activity, the associated immunity proteins only provide protection against their cognate toxins.

Purified CdiA-CT^{ECL} and CdiA-CT^{EC16} Cleave 16S rRNA In Vitro

In principle, CdiA-CT^{ECL} and CdiA-CT^{EC16} could induce an endogenous nuclease activity that actually catalyzes 16S rRNA cleavage. Therefore, we tested purified toxins for nuclease activity in vitro. Each CdiA-CT/CdiI-His$_6$ pair was first purified as a complex. Toxins were then eluted away from immunity proteins using Ni^{2+}-affinity chromatography under denaturing conditions. Purified toxins were refolded by dialysis against non-denaturing

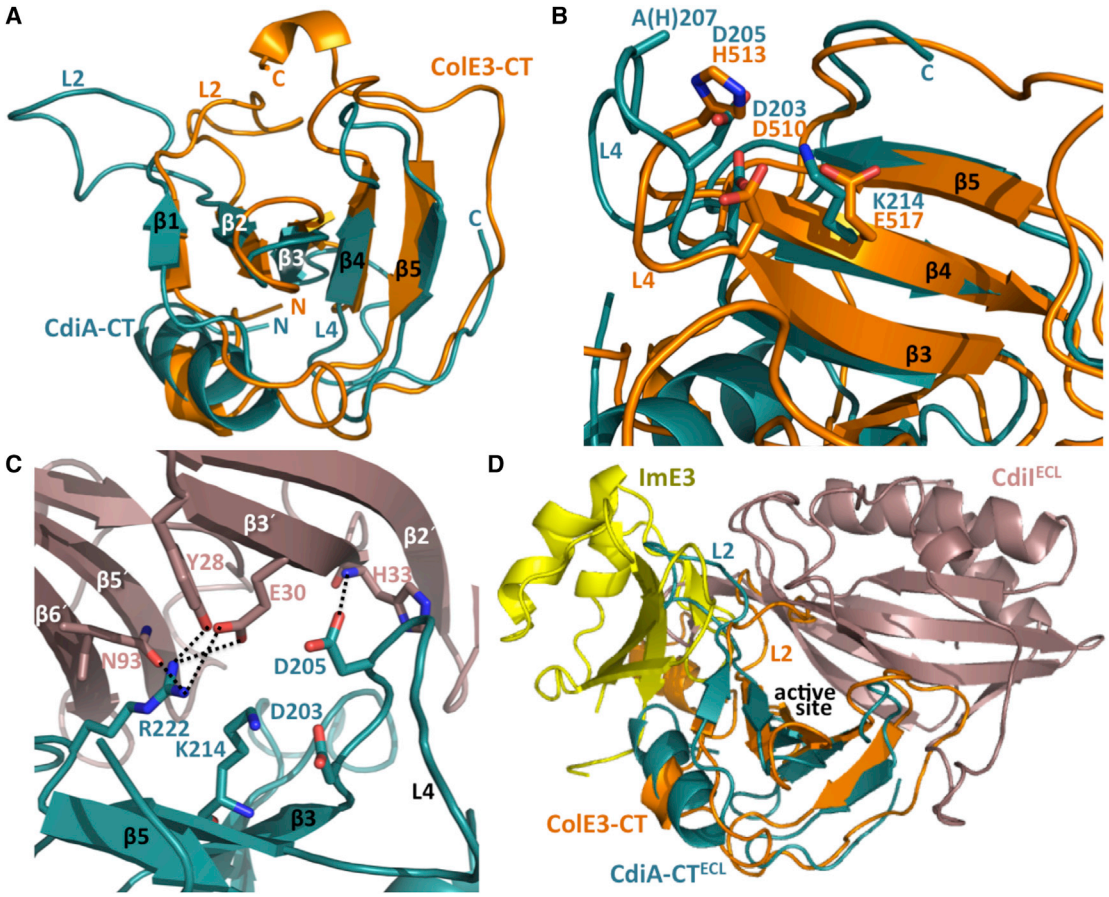

Figure 2. CdiA-CT^{ECL} Share Structural Similarities with the Nuclease Domain of Colicin E3

(A) Superimposition of CdiA-CT^{ECL} (teal) and the C-terminal nuclease domain of colicin E3 (ColE3-CT, orange) (PDB ID code 2B5U). The toxin domains superimpose with an rmsd of 2.1 Å.

(B) Colicin E3 residues Asp510, His513, and E517 are involved in catalysis and superimpose with residues Asp203, Asp205, and Lys214 of CdiA-CT^{ECL}. His207 of CdiA-CT^{ECL} is located within disordered loop L4 and is modeled as an alanine residue. Residues are indicated in one-letter code and rendered as stick representations.

(C) The predicted CdiA-CT^{ECL} active site is occluded by bound CdiI^{ECL}. Interacting bonds are represented by black dotted lines.

(D) Superimposition of CdiA-CT/CdiI^{ECL} with the ColE3-CT/ImE3 complex. Ribbon representations of CdiA-CT^{ECL} (teal), CdiI^{ECL} (salmon pink), ColE3-CT (orange), and ImE3 (yellow) are depicted.

Also see Figures S2 and S3.

buffer prior to activity assays. Before testing nuclease activity, we first confirmed that each refolded CdiA-CT is able to rebind its cognate immunity protein. We mixed CdiI-His$_6$ with either cognate or non-cognate toxin and subjected the mixtures to Ni^{2+}-affinity chromatography under non-denaturing conditions. Each CdiA-CT copurified with its cognate immunity protein (Figure 4A), indicating that the toxins can re-establish specific binding interactions after denaturation and refolding. We next treated ribosomes with purified toxins and analyzed the reactions by northern blot hybridization. Both CdiA-CT^{ECL} and CdiA-CT^{EC16} cleave a 3′-fragment from 16S rRNA, and the activity of each toxin is effectively blocked by equimolar cognate CdiI protein (Figure 4B). These results indicate that each toxin is directly responsible for 16S rRNA cleavage.

Next, we used primer extension to determine whether the CDI toxins cleave 16S rRNA at the same position as colicin E3. We generated an oligonucleotide that hybridizes to residues C1501–C1521 of *E. coli* 16S rRNA (Figure 5A) and used it as a primer in reverse transcription reactions to screen for cleavage sites. Residue U1498 of 16S rRNA is methylated at the N3 position (Figure 5A), and this modified base is predicted to interfere with reverse transcription. Therefore, we repeated the in vitro nuclease reactions using ribosomes isolated from an *E. coli* Δ*rsmE::kan* mutant, which lacks the U1498 methyltransferase (Basturea et al., 2006). Analysis of these nuclease reactions shows a strong primer-extension arrest corresponding to residue G1494 (Figures 5A and 5B). This primer extension product is neither observed when ribosomes are mock-treated with buffer nor when the reactions contain equimolar cognate CdiI protein (Figure 5B). These data are consistent with CdiA-CT-mediated cleavage of the phosphodiester bond linking residues A1493 and G1494 (Figure 5A). Thus, CdiA-CT^{ECL} and CdiA-CT^{EC16} both appear to cleave 16S rRNA at the same site as colicin E3.

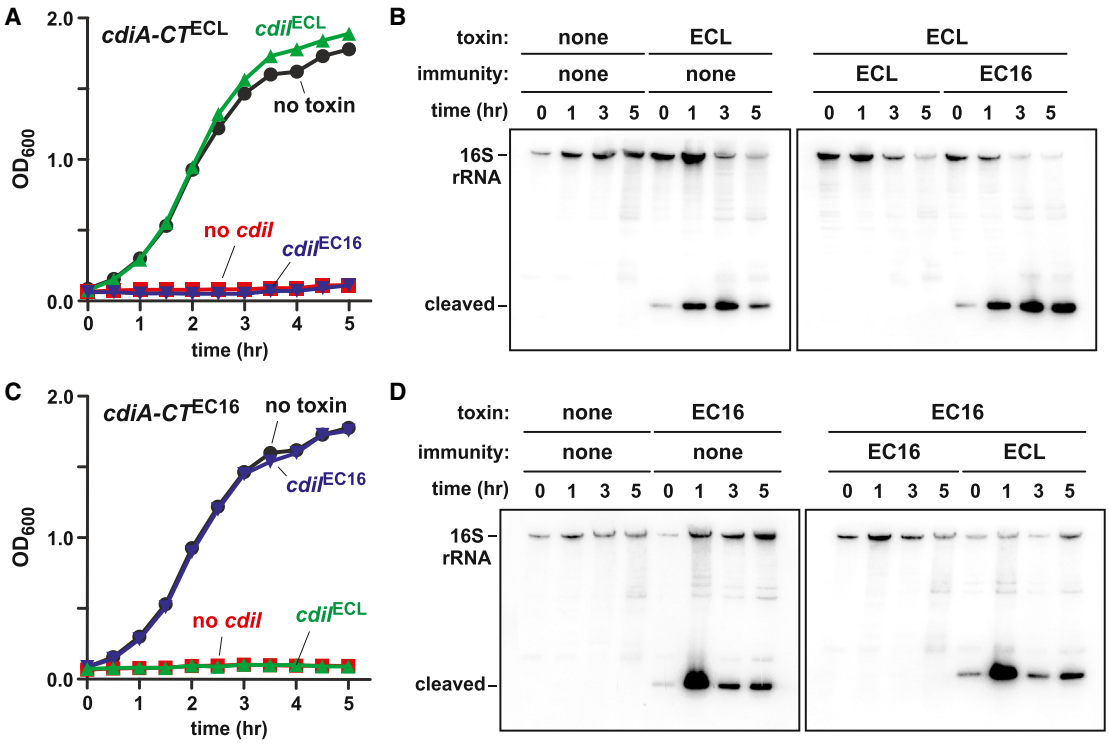

Figure 3. CdiA-CT Toxin Activity In Vivo

(A) *cdiA-CT*^{ECL} expression was induced at 0 hr, and cell growth was monitored by measuring the culture optical density at 600 nm (OD_{600}). Red curves are from cells that lack an immunity gene; the green and blue curves represent cells that express *cdiI*^{ECL} and *cdiI*^{EC16}, respectively. The black curve shows cell growth in the absence of toxin expression.

(B) Total RNA was isolated from the cells in (A) and analyzed by northern blot using a probe to the 3′-end of *E. coli* 16S rRNA. Toxin and immunity genes are indicated as ECL for *E. cloacae* and EC16 for *E. chrysanthemi* EC16. The migration positions of full-length and cleaved 16S rRNA are indicated.

(C) *cdiA-CT*^{EC16} expression was induced and cell growth monitored as outlined in (A).

(D) RNA was isolated from the cells in (C) and analyzed as described for (B).

Also see Figure S4.

Mutational Analysis Confirms Active-Site Residues Identified in the CdiA-CT^{ECL} Structure

The side chains of CdiA-CT^{ECL} Asp203 and Lys214 overlay with active-site residues Asp510 and Glu517 (respectively) of colicin E3 (Figures 2B and S2A). However, because loop L4 is not well resolved in the CdiA-CT^{ECL} structure, it is difficult to unambiguously identify a catalytic residue corresponding to His513 of colicin E3. Therefore, we mutated CdiA-CT^{ECL} residues Asp203, Asp205, His207, and Lys214 individually to alanine and tested the resulting proteins for toxicity in vivo and 16S rRNase activity in vitro. CdiA-CT^{ECL} variants containing Asp203Ala, His207Ala, or Lys214Ala mutations have no effect on *E. coli* cell growth (Figure 6A), suggesting that nuclease activity is disrupted. The Asp205Ala variant shows a delayed inhibition phenotype, in which cell growth is arrested ~90 min after toxin expression is induced (Figure 6A). Comparable results were obtained with in vitro reactions using purified toxin variants. CdiA-CT^{ECL} carrying the Asp203Ala, His207Ala, and Lys214Ala mutations has no detectable rRNase activities in vitro, whereas the Asp205Ala variant exhibits lower activity than the wild-type enzyme (Figure 6B). We note that all CdiA-CT^{ECL} variants appear to be folded properly, because each protein efficiently rebinds cognate CdiI^{ECL} immunity protein in vitro (Figure 6C). Together, these experiments indicate that Asp203, His207, and Lys214 are required for toxin activity and could function in catalysis, whereas Asp205 plays an important, yet non-essential, role.

CdiA-CT^{ECL} Is Delivered into Target Bacteria during CDI

Next, we asked whether the *E. cloacae* CDI system is expressed and deployed for competition. We reasoned that *E. cloacae* mutants lacking the immunity gene should be susceptible to inhibition. We deleted the *cdiA*^{ECL} and *cdiI*^{ECL} genes and tested the resulting double mutant strain in competition cocultures with wild-type *E. cloacae* cells. We found that the *E. cloacae* Δ*cdiA*^{ECL} Δ*cdiI*^{ECL} mutants are not inhibited by wild-type cells in either liquid or solid media (Figure 7A, gray bars; data not shown), suggesting that the CDI^{ECL} system is not functional or may not be expressed under laboratory conditions. Therefore, we introduced the *E. coli araBAD* promoter upstream of the *E. cloacae cdi* locus to allow inducible expression and used this inhibitor strain for competitions on solid growth media. When the CDI^{ECL} system is induced, the growth of target cells is suppressed approximately 20-fold compared to cocultures with *E. cloacae* cells carrying the wild-type *cdi* locus (Figure 7A, compare white to gray bars). Moreover, target cell growth is restored if they

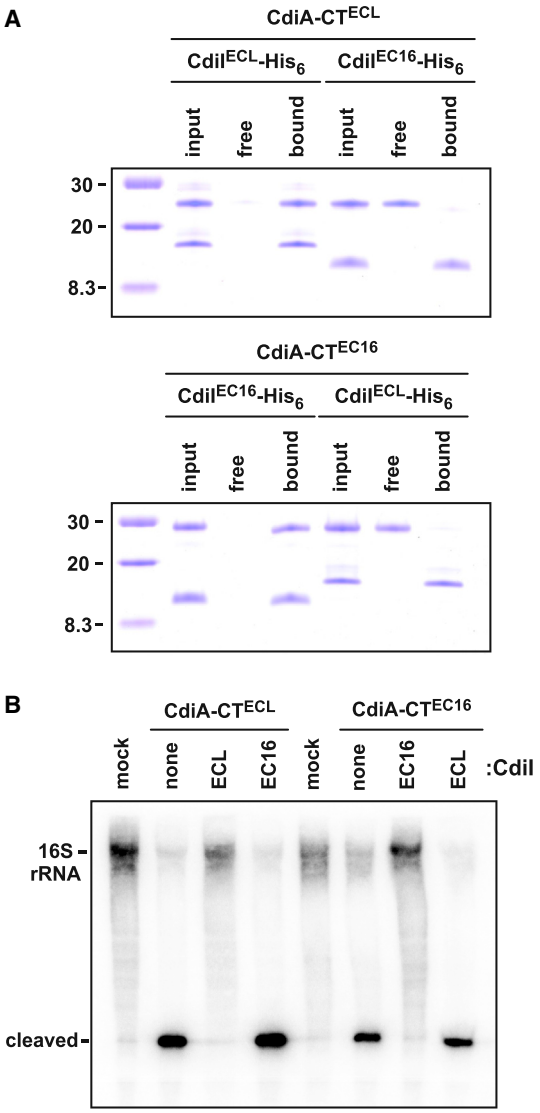

Figure 4. CdiA-CT Toxin Activity In Vitro

(A) Purified CdiA-CT toxins and CdiI-His_6 immunity proteins were mixed and then subjected to Ni^{2+}-affinity chromatography under non-denaturing conditions. Lanes labeled input represent CdiA-CT/CdiI-His_6 mixtures prior to chromatography; lanes labeled free are proteins that fail to bind Ni^{2+}-resin; and lanes labeled bound are proteins that elute with imidazole.

(B) Isolated *E. coli* ribosomes were treated with purified CdiA-CT^{ECL} and CdiA-CT^{EC16}, and the reactions analyzed by northern blot using a probe to the 3′-end of 16S rRNA. Where indicated, CdiI-His_6^{ECL} (ECL) or CdiI-His_6^{EC16} (EC16) was added at an equimolar ratio to the toxin. Mock reactions are ribosome samples that were treated with buffer. The migration positions of full-length and cleaved 16S rRNA are indicated.

carry a plasmid-borne copy of the *cdiI*^{ECL} immunity gene, but the non-cognate *cdiI*^{EC16} gene provides no protection (Figure 7A). We also tested the inducible *E. cloacae* inhibitor cells in cocultures with *E. coli* target cells. Because *E. cloacae* ATCC 13047 uses one of its type VI secretion systems to inhibit *E. coli* (Ruhe et al., 2013b), we first deleted the *tssM1* gene (ECL_01536) from the *E. cloacae* inhibitor strain to inactivate type VI secretion. Remarkably, *E. coli* cells are more sensitive to growth inhibition, with viable target cell counts reduced ~100-fold after 4 hr of coculture (Figure 7B). Notably, *E. coli* cell growth is unaffected during coculture with *E. cloacae* containing the wild-type *cdi* locus (Figure 7B), again indicating that the CDI^{ECL} system is not expressed on lab media. Moreover, *E. coli* targets are protected by plasmid-borne *cdiI*^{ECL}, but not by *cdiI*^{EC16} (Figure 7B), confirming that growth inhibition is due to CdiA-CT^{ECL} toxin activity.

Many CdiA-CT toxins are modular and can be exchanged between different CdiA proteins to generate functional effector molecules (Aoki et al., 2010; Morse et al., 2012; Nikolakakis et al., 2012; Webb et al., 2013). To test whether the CdiA-CT/CdiI^{ECL} toxin/immunity protein complex is functional in the context of another CDI system, we replaced the *cdiA-CT*/*cdiI*^{EC93} region of the *E. coli* EC93 CDI system with the *E. cloacae* toxin/immunity coding sequences. This fusion produces a chimeric CdiA protein with CdiA-CT^{ECL} grafted onto $CdiA^{EC93}$ at the VENN peptide motif. *E. coli* cells expressing the *cdiA*^{EC93}-*CT*^{ECL} chimera are potent inhibitors, capable of reducing viable *E. coli* target cells ~10^4-fold after 3 hr of coculture (Figure 8A). Again, target cells that carry the *cdiI*^{ECL} immunity gene are not inhibited and grow to the same level as cells cultured with mock-inhibitor cells that lack a CDI system (Figure 8A). However, target cells expressing non-cognate *cdiI*^{EC16} are inhibited to the same extent as cells that carry no immunity gene (Figure 8A). Because the inhibition effect is so profound in these co-culture experiments, we asked whether toxin-damaged ribosomes could be detected in the target cells. We isolated total RNA from each competition coculture and performed northern blot analysis to assay for RNase activity. Cleaved 16S rRNA is readily detected when the target cells lack immunity or express non-cognate *cdiI*^{EC16} immunity, but this nuclease activity is not observed when target cells carry the cognate *cdiI*^{ECL} gene (Figure 8B). We also generated and tested inhibitor cells that express chimeric *cdiA*^{EC93}-*CT*^{ECL} containing the His207Ala active-site mutation. Cells expressing the mutant effector do not inhibit *E. coli* targets, and no 16S rRNA cleavage is detected in the competition coculture (Figures 8A and 8B). Together, these results demonstrate that the CdiA-CT^{ECL} toxin is delivered into target bacteria during CDI and that 16S RNase activity is solely responsible for growth inhibition.

DISCUSSION

CdiA proteins carry a variety of sequence-diverse C-terminal domains, which represent a collection of distinct toxins. Determining the biochemical activities of so many different toxins remains an important problem in the field (Aoki et al., 2010; Ruhe et al., 2013a). Zhang et al. (2012) have successfully used comparative sequence analyses to predict that many CdiA-CT toxins have nuclease activities. However, these predictions often do not identify specific nucleic acid substrates and may be inaccurate in some instances. In fact, the current annotation for CdiA-CT^{ECL} (Pfam PF15526; http://pfam.sanger.ac.uk/family/Toxin_46) suggests that this toxin adopts a Barnase-EndoU-colicin E5/RelE (BECR) protein fold and targets tRNA molecules for cleavage. The work presented here demonstrates that CdiA-CT^{ECL} is actually most similar to the C-terminal nuclease

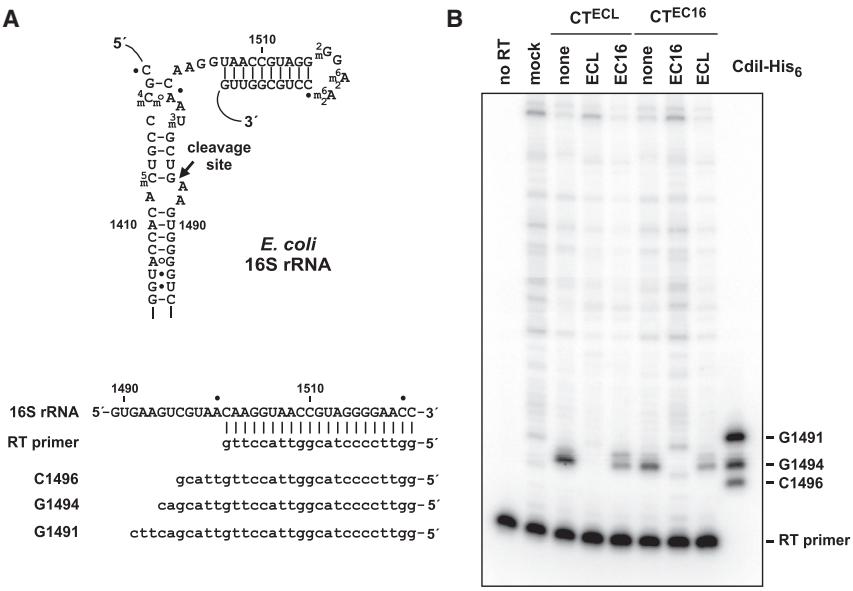

Figure 5. CdiA-CT^{ECL} and CdiA-CT^{EC16} Cleave 16S rRNA between A1393 and G1394

(A) Nucleotide sequence and secondary structure of the 30S subunit decoding center. The sequence of the reverse transcription (RT) primer is shown in heteroduplex with its complementary sequence in 16S rRNA. Oligonucleotides C1496, G1494, and G1491 were used as gel migration standards. The 16S rRNA cleavage site is indicated by an arrow.

(B) Ribosomal RNA was extracted from the indicated in vitro nuclease reactions and hybridized to radiolabeled RT primer for primer extension analysis using reverse transcriptase. Reactions were resolved on a denaturing gel and visualized by phosphorimaging. The migration positions of oligonucleotides C1496, G1494, and G1491 are indicated.

domain of colicin E3. Consistent with this structural homology, CdiA-CT^{ECL} is a site-specific 16S rRNase rather than a tRNase. Furthermore, we note that even accurate protein-fold predictions can lead to erroneous assignments of biochemical activity. For example, CdiA-CT^{Bp1026b} from *B. pseudomallei* 1026b has the same fold as type IIS restriction endonucleases, yet this toxin is a specific tRNase and has no detectable DNase activity (Morse et al., 2012; Nikolakakis et al., 2012). These discrepancies between prediction and experimental characterization underscore the need for careful biochemical analysis to test sequence-based hypotheses.

The activity of colicin E3 was first described over 40 years ago (Bowman et al., 1971; Senior and Holland, 1971), yet a catalytic mechanism has only recently been proposed based on the structure of the enzyme bound to the ribosome (Ng et al., 2010). The mechanistic model postulates that Glu517 of colicin E3 acts as a general base to abstract a proton from the 2′-OH of 16S rRNA residue A1493. The resulting alkoxide subsequently attacks the phosphodiester linking A1493 and G1494 to cleave the 16S rRNA chain. The side chain of His513 is thought to stabilize the transition state as well as donate a proton to the 5′-OH leaving group after cleavage. Colicin E3 residues Asp510 and Glu515 are within H-bonding distance of His513 and may promote protonation of its imidazole ring (Ng et al., 2010). Comparative structure analysis suggests that residues Asp203, Asp205, and Lys214 of CdiA-CT^{ECL} are involved in catalysis because they are in the same relative positions as Asp510, His513, and Glu517 (respectively) of colicin E3. The superimposition of these residues is remarkable given that loop L4 of CdiA-CT^{ECL}, which contains the predicted active-site residues, is significantly longer and more flexible than the corresponding region in colicin E3 (see Figure 2A). Mutagenesis experiments confirm that these CdiA-CT^{ECL} residues are important for nuclease activity, but it is not clear that the two enzymes share the same catalytic mechanism. For example, Lys214 in CdiA-CT^{ECL} is unlikely to function as a generalized base as proposed for Glu517 of ColE3-CT, especially as nearby residues Asp203 and Asp205 within CdiA-CT^{ECL} should favor protonation of Lys214. Lysine residues are often found in the active sites of nucleases and typically function to position the scissile phosphodiester or stabilize pentavalent transition states (Gite et al., 1992; Pingoud and Jeltsch, 2001; Richardson et al., 1990). Therefore, it seems likely that Lys214 serves one of the aforementioned functions, leaving His207 to act as the general base that initiates 16S rRNA cleavage. Though we have no structural information for CdiA-CT^{ECL} bound to the ribosome, the available data suggest that colicin E3 and CdiA-CT^{ECL} probably utilize distinct catalytic strategies.

The lack of sequence identity between CdiA-CT^{ECL} and ColE3-CT also raises questions about how the CDI toxin binds to the ribosome. Ng et al. (2010) have shown that ColE3-CT loop L2 makes a number of specific contacts with the ribosome A site. Residues Arg495 and Gln489 bind the nucleobase and phosphate of 16S rRNA residue A1493; Lys496 interacts with C518; and Lys494 holds G530 in the *syn* conformation through a bridging water molecule (Ng et al., 2010). These toxin residues are highly conserved between colicins E3, E4, and E6 and cloacin DF, suggesting that these enzymes all bind the ribosome in the same manner. By contrast, not one of these loop L2 residues is shared with CdiA-CT^{ECL} (see Figure S2A). In fact, loop L2 of CdiA-CT^{ECL} is significantly displaced compared to ColE3-CT. This displacement may result from the binding of CdiI^{ECL}, which would clash with loop L2 if it were in the ColE3-CT conformation. In the absence of CdiI^{ECL}, it is possible that loop L2 of CdiA-CT^{ECL} adopts the same conformation seen in ColE3-CT, but the sequence divergence suggests that each loop makes distinct contacts with the ribosome. ColE3-CT makes additional contacts with ribosomal protein S12 within the A site. Residues Tyr460–Tyr464 form an intriguing pseudo-β sheet interaction with the side chains from His462, Asp463, and Tyr464, making specific H-bond contacts with S12 (Ng et al., 2010). Unfortunately, the corresponding region of CdiA-CT^{ECL} was degraded during crystallization, precluding a direct comparison of these structures. But again, the primary sequences in this region share no obvious homology, indicating that the two toxins probably interact with ribosomal protein S12 in distinct manners.

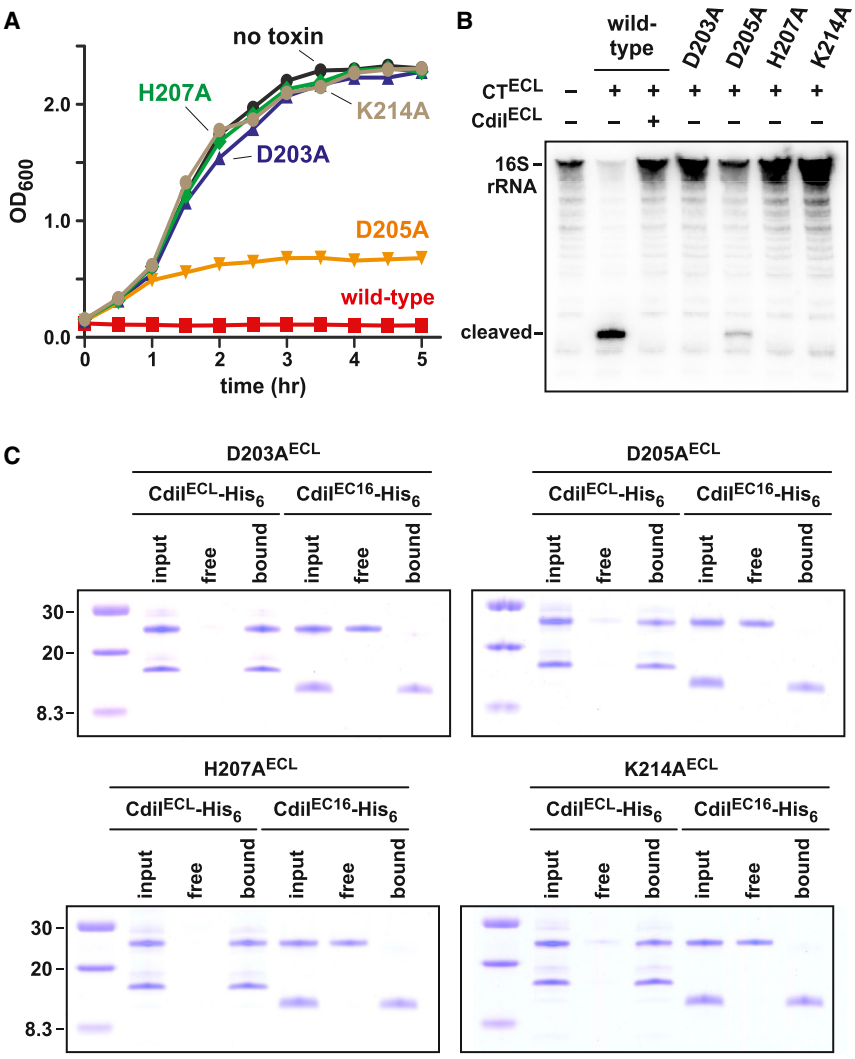

Figure 6. Mutagenesis of Predicted Active-Site Residues in CdiA-CT^{ECL}

(A) Expression of *cdiA-CT*^{ECL} and the indicated mutated variants were induced at 0 hr with L-arabinose and cell growth monitored by measuring the optical density of the culture at 600 nm (OD_{600}). The black curve shows the growth of a control culture without toxin expression.

(B) Isolated *E. coli* ribosomes were treated with purified CdiA-CT^{ECL} toxins and RNA extracted for northern blot analysis. Where indicated, purified CdiI-His$_6$^{ECL} was included in the reaction. The gel migration positions of full-length and cleaved 16S rRNA are indicated.

(C) Purified CdiA-CT toxins and CdiI-His$_6$ immunity proteins were mixed and then subjected to Ni^{2+}-affinity chromatography under non-denaturing conditions. Lanes labeled input represent CdiA-CT/CdiI-His$_6$ mixtures prior to chromatography; lanes labeled free are proteins that fail to bind Ni^{2+}-resin; and lanes labeled bound are proteins that elute with imidazole.

Finally, we note that there are several fundamental differences between CdiI^{ECL} and ImE3 immunity proteins. CdiI^{ECL} and ImE3 differ significantly in molecular mass, share less than 12% sequence identity, and bind to non-overlapping sites on their cognate nuclease domains. Moreover, each immunity protein has a distinct tertiary structure and fold. Structural homology searches reveal that CdiI^{ECL} is most similar to the Whirly family of single-stranded DNA-binding proteins. Although this homology is relatively weak (*Z* scores 4.1 to 4.3 and rmsd ~4.0 Å), CdiI^{ECL} shares a characteristic topology with all Whirly proteins (see Figure S3B). The fact that the immunity proteins for colicin E3 and CdiA-CT^{ECL} toxins are unrelated in both primary sequence and tertiary structure suggests that these toxin-immunity pairs have independent origins. Because cognate toxin/immunity gene pairs are closely linked, they must presumably coevolve as a unit. This process is thought to involve initial changes in the immunity protein, followed by compensatory mutations in the toxin that restore high-binding affinity between the two proteins (Riley, 1993; Tan and Riley, 1997). In general, there are few constraints to impede the drift of immunity genes, because they need only encode proteins that bind toxins. By contrast, toxins are often enzymes and must retain the ability to bind substrates and catalyze reactions. This model is largely supported by analyses showing that immunity proteins diverge more rapidly than do toxins (Ruhe et al., 2013a; Tan and Riley, 1997). Thus, although it is formally possible that ImE3 and CdiI^{ECL} arose from a common ancestor, the differences in immunity protein folds make this model much less likely. Based on this reasoning, we speculate that CdiA-CT^{ECL}/CdiI^{ECL} and ColE3-CT/ImE3 evolved from different lineages and that the structural and enzymatic similarities between the toxins reflect convergent evolution.

EXPERIMENTAL PROCEDURES

Bacterial Strains, Plasmids, and Growth Conditions

All bacterial strains and plasmids used in this study are listed in Table S2. Bacteria were grown in lysogeny broth media or LB-agar with the appropriate antibiotics as described in the Supplemental Experimental Procedures. *E. cloacae* genes were deleted using the same protocol as that described for *E. coli* (Hayes et al., 2002). DNA sequences located upstream and downstream of target genes were amplified and cloned into plasmid pKAN or pSPM (Koskiniemi et al., 2013) to flank kanamycin or spectinomycin resistance cassettes, respectively. The resulting plasmids were linearized by restriction endonuclease digestion and electroporated into *E. cloacae* cells expressing the phage λ Red proteins from plasmid pKOBEG (Pérez et al., 2007). The details of all strain and plasmid constructions are provided in the Supplemental Experimental Procedures.

Protein Purification and Crystallography

CdiA-CT/CdiI-His$_6$ complexes were purified and the toxin and immunity proteins isolated from one another as described previously (Diner et al., 2012; Nikolakakis et al., 2012). The CdiA-CT/CdiI^{ECL} complex was crystallized

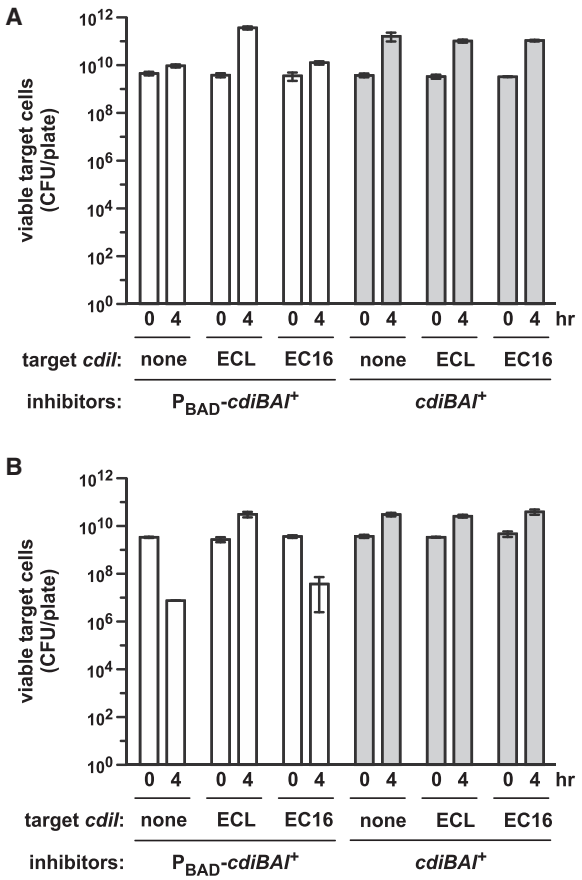

Figure 7. Intercellular Competitions with *E. cloacae* Inhibitor Cells

(A) Intra-species competition. *E. cloacae* inhibitor cells were cocultured with *E. cloacae* Δ*cdiA*^{ECL} Δ*cdiI*^{ECL} target cells on LB-agar supplemented with arabinose. Where indicated, target cells were provided with plasmid-borne *cdiI*^{ECL} or *cdiI*^{EC16} immunity genes. Total viable target cells were determined as colony-forming units. White bars correspond to competitions with arabinose-inducible inhibitor cells (P_{BAD}-*cdiBAI*$^+$), and gray bars correspond to competitions with inhibitors that carry the wild-type locus (*cdiBAI*$^+$).

(B) Inter-species competition. *E. cloacae* inhibitor cells were cocultured with *E. coli* target cells on LB-agar supplemented with arabinose. Where indicated, the target cells were provided with plasmid-borne *cdiI*^{ECL} or *cdiI*^{EC16} immunity genes. Viable target cells were determined as colony-forming units (CFU), and data are reported as the mean ± SEM for two independent experiments.

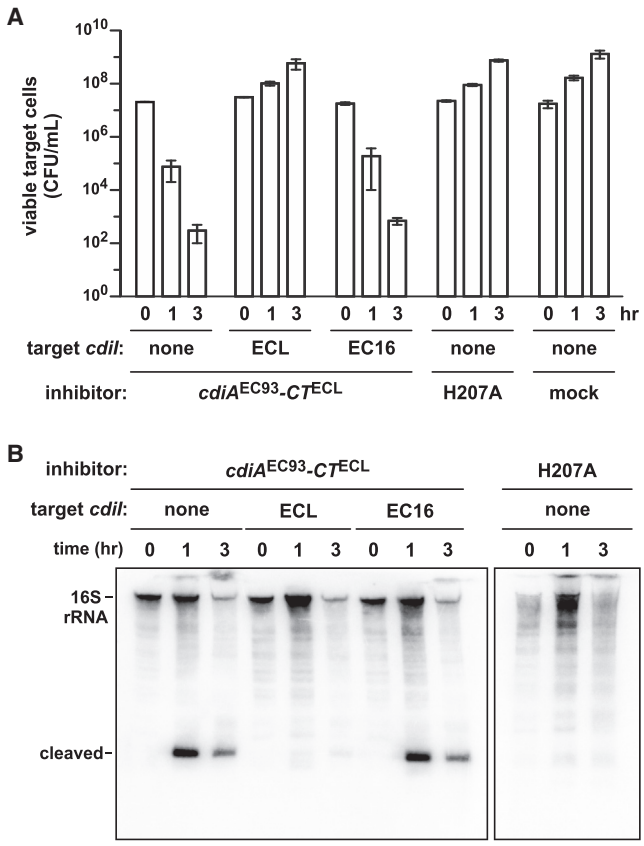

Figure 8. The CdiA-CT^{ECL} Toxin Domain Is Modular

(A) *E. coli* target cells were cocultured with inhibitor cells that express chimeric CdiA^{EC93}-CT^{ECL} in broth. Where indicated, target cells were provided with plasmid-borne copies of the *cdiI*^{ECL} or *cdiI*^{EC16} immunity genes. The inhibitors labeled H207A express CdiA^{EC93}-CT^{ECL} containing the His207Ala mutation in the toxin domain. Mock inhibitors lack the CDI system. Viable target cell counts were determined as CFU/ml, and data are reported as the mean ± SEM for two independent experiments.

(B) Total RNA was isolated from the co-culture experiments described in (A) and analyzed by northern blot using a probe to the 3′-end of 16S rRNA.

as described previously (Goulding and Perry, 2003). Crystals were grown at room temperature by hanging drop-vapor diffusion with a reservoir containing 1.5 M $(NH_4)_2SO_4$, 0.1 M Bis Tris (pH 5.1), and 1% (wt/vol) PEG 3350. The structural model was determined as described previously (Morse et al., 2012). Non-optimal detector positioning during data collection necessitated the high-resolution limit of 2.4 Å. All crystallography and refinement statistics are presented in Table 1. Atomic coordinates and structure factors have been deposited in the PDB (http://www.pdb.org) with the ID code 4NTQ.

Nuclease Assays

Ribosomes were isolated from S30 lysates of *E. coli* as described (Diner and Hayes, 2009) and incubated with purified CdiA-CT toxins and CdiI immunity proteins as described in the Supplemental Experimental Procedures. All reactions were analyzed by northern blot using a probe complementary to the 3′-end of *E. coli* 16S rRNA. CdiA-CT cleavage sites were determined using ribosomes from *E. coli* Δ*rsmE* cells. Reactions were quenched with guanidinium isothiocyanate-phenol and rRNA extracted for primer extension analysis as described previously (Diner and Hayes, 2009).

Growth Competitions

E. cloacae inhibitor cells were cocultured with *E. cloacae* Δ*cdiAI* target cells on LB-agar supplemented with 0.2% L-arabinose. Cells were harvested and enumerated as colony-forming units (CFU). Immunity function was evaluated through expression of *cdiI* genes in target cells from plasmid constructs as described in the supplement. Cross-species competitions were performed under the same conditions using *E. coli* target cells. Chimeric EC93-ECL CDI systems were expressed from cosmids in *E. coli* EPI100. Inhibitor cells were cocultured with target cells in LB media. Samples were taken for enumeration of viable target cells. *E. coli* EPI100 cells carrying cosmid pWEB-TNC were used as mock (CDI$^-$) inhibitors.

ACCESSION NUMBERS

Atomic coordinates and structure factors have been deposited in the Protein Data Bank (http://www.pdb.org) with the ID code 4NTQ.

SUPPLEMENTAL INFORMATION

Supplemental Information includes Supplemental Experimental Procedures, four figures, and two tables and can be found with this article online at http://dx.doi.org/10.1016/j.str.2014.02.012.

ACKNOWLEDGMENTS

This work was supported by grants from the National Institutes of Health (R21 AI099687 to C.S.H. and C.W.G. and U01 GM102318 to D.A.L., C.S.H., and C.W.G.). For their invaluable help with data collection, we thank the staff at both the Advanced Light Source (U.S. Department of Energy under contract no. DE-AC02-05CH11231) at Berkeley National Laboratories and the Stanford Synchrotron Radiation Lightsource (supported in part by P41 GM103393). The funders had no role in the study design, data collection and analysis, decision to publish, or preparation of the manuscript.

Received: December 19, 2013
Revised: February 11, 2014
Accepted: February 16, 2014
Published: March 20, 2014

REFERENCES

Aoki, S.K., Pamma, R., Hernday, A.D., Bickham, J.E., Braaten, B.A., and Low, D.A. (2005). Contact-dependent inhibition of growth in *Escherichia coli*. Science *309*, 1245–1248.

Aoki, S.K., Malinverni, J.C., Jacoby, K., Thomas, B., Pamma, R., Trinh, B.N., Remers, S., Webb, J., Braaten, B.A., Silhavy, T.J., and Low, D.A. (2008). Contact-dependent growth inhibition requires the essential outer membrane protein BamA (YaeT) as the receptor and the inner membrane transport protein AcrB. Mol. Microbiol. *70*, 323–340.

Aoki, S.K., Diner, E.J., de Roodenbeke, C.T., Burgess, B.R., Poole, S.J., Braaten, B.A., Jones, A.M., Webb, J.S., Hayes, C.S., Cotter, P.A., and Low, D.A. (2010). A widespread family of polymorphic contact-dependent toxin delivery systems in bacteria. Nature *468*, 439–442.

Basturea, G.N., Rudd, K.E., and Deutscher, M.P. (2006). Identification and characterization of RsmE, the founding member of a new RNA base methyltransferase family. RNA *12*, 426–434.

Bowman, C.M., Dahlberg, J.E., Ikemura, T., Konisky, J., and Nomura, M. (1971). Specific inactivation of 16S ribosomal RNA induced by colicin E3 in vivo. Proc. Natl. Acad. Sci. USA *68*, 964–968.

Carr, S., Walker, D., James, R., Kleanthous, C., and Hemmings, A.M. (2000). Inhibition of a ribosome-inactivating ribonuclease: the crystal structure of the cytotoxic domain of colicin E3 in complex with its immunity protein. Structure *8*, 949–960.

Cascales, E., Buchanan, S.K., Duché, D., Kleanthous, C., Lloubès, R., Postle, K., Riley, M., Slatin, S., and Cavard, D. (2007). Colicin biology. Microbiol. Mol. Biol. Rev. *71*, 158–229.

Chao, L., and Levin, B.R. (1981). Structured habitats and the evolution of anticompetitor toxins in bacteria. Proc. Natl. Acad. Sci. USA *78*, 6324–6328.

Czárán, T.L., Hoekstra, R.F., and Pagie, L. (2002). Chemical warfare between microbes promotes biodiversity. Proc. Natl. Acad. Sci. USA *99*, 786–790.

Desveaux, D., Maréchal, A., and Brisson, N. (2005). Whirly transcription factors: defense gene regulation and beyond. Trends Plant Sci. *10*, 95–102.

Diner, E.J., and Hayes, C.S. (2009). Recombineering reveals a diverse collection of ribosomal proteins L4 and L22 that confer resistance to macrolide antibiotics. J. Mol. Biol. *386*, 300–315.

Diner, E.J., Beck, C.M., Webb, J.S., Low, D.A., and Hayes, C.S. (2012). Identification of a target cell permissive factor required for contact-dependent growth inhibition (CDI). Genes Dev. *26*, 515–525.

Gite, S., Reddy, G., and Shankar, V. (1992). Active-site characterization of S1 nuclease. I. Affinity purification and influence of amino-group modification. Biochem. J. *285*, 489–494.

Gordon, D.M., Riley, M.A., and Pinou, T. (1998). Temporal changes in the frequency of colicinogeny in *Escherichia coli* from house mice. Microbiology *144*, 2233–2240.

Goulding, C.W., and Perry, L.J. (2003). Protein production in *Escherichia coli* for structural studies by X-ray crystallography. J. Struct. Biol. *142*, 133–143.

Hayes, C.S., Bose, B., and Sauer, R.T. (2002). Proline residues at the C terminus of nascent chains induce SsrA tagging during translation termination. J. Biol. Chem. *277*, 33825–33832.

Holberger, L.E., Garza-Sánchez, F., Lamoureux, J., Low, D.A., and Hayes, C.S. (2012). A novel family of toxin/antitoxin proteins in *Bacillus* species. FEBS Lett. *586*, 132–136.

Holm, L., and Rosenström, P. (2010). Dali server: conservation mapping in 3D. Nucleic Acids Res. *38* (Web Server issue), W545–W549.

Hood, R.D., Singh, P., Hsu, F., Güvener, T., Carl, M.A., Trinidad, R.R., Silverman, J.M., Ohlson, B.B., Hicks, K.G., Plemel, R.L., et al. (2010). A type VI secretion system of *Pseudomonas aeruginosa* targets a toxin to bacteria. Cell Host Microbe *7*, 25–37.

Koskiniemi, S., Lamoureux, J.G., Nikolakakis, K.C., t'Kint de Roodenbeke, C., Kaplan, M.D., Low, D.A., and Hayes, C.S. (2013). Rhs proteins from diverse bacteria mediate intercellular competition. Proc. Natl. Acad. Sci. USA *110*, 7032–7037.

Lancaster, L.E., Savelsbergh, A., Kleanthous, C., Wintermeyer, W., and Rodnina, M.V. (2008). Colicin E3 cleavage of 16S rRNA impairs decoding and accelerates tRNA translocation on *Escherichia coli* ribosomes. Mol. Microbiol. *69*, 390–401.

MacIntyre, D.L., Miyata, S.T., Kitaoka, M., and Pukatzki, S. (2010). The *Vibrio cholerae* type VI secretion system displays antimicrobial properties. Proc. Natl. Acad. Sci. USA *107*, 19520–19524.

Morse, R.P., Nikolakakis, K.C., Willett, J.L., Gerrick, E., Low, D.A., Hayes, C.S., and Goulding, C.W. (2012). Structural basis of toxicity and immunity in contact-dependent growth inhibition (CDI) systems. Proc. Natl. Acad. Sci. USA *109*, 21480–21485.

Ng, C.L., Lang, K., Meenan, N.A., Sharma, A., Kelley, A.C., Kleanthous, C., and Ramakrishnan, V. (2010). Structural basis for 16S ribosomal RNA cleavage by the cytotoxic domain of colicin E3. Nat. Struct. Mol. Biol. *17*, 1241–1246.

Nikolakakis, K., Amber, S., Wilbur, J.S., Diner, E.J., Aoki, S.K., Poole, S.J., Tuanyok, A., Keim, P.S., Peacock, S., Hayes, C.S., and Low, D.A. (2012). The toxin/immunity network of *Burkholderia pseudomallei* contact-dependent growth inhibition (CDI) systems. Mol. Microbiol. *84*, 516–529.

Ogawa, T., Tomita, K., Ueda, T., Watanabe, K., Uozumi, T., and Masaki, H. (1999). A cytotoxic ribonuclease targeting specific transfer RNA anticodons. Science *283*, 2097–2100.

Pérez, A., Canle, D., Latasa, C., Poza, M., Beceiro, A., Tomás, Mdel.M., Fernández, A., Mallo, S., Pérez, S., Molina, F., et al. (2007). Cloning, nucleotide sequencing, and analysis of the AcrAB-TolC efflux pump of *Enterobacter cloacae* and determination of its involvement in antibiotic resistance in a clinical isolate. Antimicrob. Agents Chemother. *51*, 3247–3253.

Pingoud, A., and Jeltsch, A. (2001). Structure and function of type II restriction endonucleases. Nucleic Acids Res. *29*, 3705–3727.

Poole, S.J., Diner, E.J., Aoki, S.K., Braaten, B.A., t'Kint de Roodenbeke, C., Low, D.A., and Hayes, C.S. (2011). Identification of functional toxin/immunity genes linked to contact-dependent growth inhibition (CDI) and rearrangement hotspot (Rhs) systems. PLoS Genet. *7*, e1002217.

Richardson, R.M., Parés, X., and Cuchillo, C.M. (1990). Chemical modification by pyridoxal 5′-phosphate and cyclohexane-1,2-dione indicates that Lys-7 and Arg-10 are involved in the p2 phosphate-binding subsite of bovine pancreatic ribonuclease A. Biochem. J. *267*, 593–599.

Riley, M.A. (1993). Positive selection for colicin diversity in bacteria. Mol. Biol. Evol. *10*, 1048–1059.

Riley, M.A., and Gordon, D.M. (1992). A survey of Col plasmids in natural isolates of *Escherichia coli* and an investigation into the stability of Col-plasmid lineages. J. Gen. Microbiol. *138*, 1345–1352.

Rojas, C.M., Ham, J.H., Deng, W.L., Doyle, J.J., and Collmer, A. (2002). HecA, a member of a class of adhesins produced by diverse pathogenic bacteria, contributes to the attachment, aggregation, epidermal cell killing, and virulence phenotypes of *Erwinia chrysanthemi* EC16 on *Nicotiana clevelandii* seedlings. Proc. Natl. Acad. Sci. USA *99*, 13142–13147.

Rojas, C.M., Ham, J.H., Schechter, L.M., Kim, J.F., Beer, S.V., and Collmer, A. (2004). The *Erwinia chrysanthemi* EC16 *hrp/hrc* gene cluster encodes an active Hrp type III secretion system that is flanked by virulence genes functionally unrelated to the Hrp system. Mol. Plant Microbe Interact. *17*, 644–653.

Ruhe, Z.C., Low, D.A., and Hayes, C.S. (2013a). Bacterial contact-dependent growth inhibition. Trends Microbiol. *21*, 230–237.

Ruhe, Z.C., Wallace, A.B., Low, D.A., and Hayes, C.S. (2013b). Receptor polymorphism restricts contact-dependent growth inhibition to members of the same species. MBio. *4*, e00480-13.

Schaller, K., and Nomura, M. (1976). Colicin E2 is DNA endonuclease. Proc. Natl. Acad. Sci. USA *73*, 3989–3993.

Senior, B.W., and Holland, I.B. (1971). Effect of colicin E3 upon the 30S ribosomal subunit of *Escherichia coli*. Proc. Natl. Acad. Sci. USA *68*, 959–963.

Silverman, J.M., Brunet, Y.R., Cascales, E., and Mougous, J.D. (2012). Structure and regulation of the type VI secretion system. Annu. Rev. Microbiol. *66*, 453–472.

Soelaiman, S., Jakes, K., Wu, N., Li, C., and Shoham, M. (2001). Crystal structure of colicin E3: implications for cell entry and ribosome inactivation. Mol. Cell *8*, 1053–1062.

Tan, Y., and Riley, M.A. (1997). Positive selection and recombination: major molecular mechanisms in colicin diversification. Trends Ecol. Evol. *12*, 348–351.

Walker, D., Lancaster, L., James, R., and Kleanthous, C. (2004). Identification of the catalytic motif of the microbial ribosome inactivating cytotoxin colicin E3. Protein Sci. *13*, 1603–1611.

Webb, J.S., Nikolakakis, K.C., Willett, J.L., Aoki, S.K., Hayes, C.S., and Low, D.A. (2013). Delivery of CdiA nuclease toxins into target cells during contact-dependent growth inhibition. PLoS ONE *8*, e57609.

Zhang, D., Iyer, L.M., and Aravind, L. (2011). A novel immunity system for bacterial nucleic acid degrading toxins and its recruitment in various eukaryotic and DNA viral systems. Nucleic Acids Res. *39*, 4532–4552.

Zhang, D., de Souza, R.F., Anantharaman, V., Iyer, L.M., and Aravind, L. (2012). Polymorphic toxin systems: Comprehensive characterization of trafficking modes, processing, mechanisms of action, immunity and ecology using comparative genomics. Biol. Direct *7*, 18.

Zheng, J., Ho, B., and Mekalanos, J.J. (2011). Genetic analysis of anti-amoebae and anti-bacterial activities of the type VI secretion system in *Vibrio cholerae*. PLoS ONE *6*, e23876.

